Doping-Induced Spectral Shifts Thwart High Temperature Superconductivity in Hole-doped $CuAlO_2$

E. R. Ylvisaker and W. E. Pickett
Department of Physics, University of California Davis, Davis, California 95616
(Dated: January 6, 2013)

The hole-doped cuprate ionic insulator $CuAlO_2$ has been predicted by Nakanishi and Katayama-Yoshida (NK) to be a candidate for a high temperature $T_c \approx 50$K superconductor. Our density functional based calculations of the hole-doped material reveal surprisingly large doping-induced shifts in spectral density as well as screening of matrix elements that were not taken into account by NK. As a result, first principles linear response electron-phonon coupling (EPC) calculations reveal net *weak coupling*, giving no appreciable superconductivity but helping to understand the excellent transparent p-type conductivity in this system. These specifically two-dimensional dipole-layer driven spectral shifts provides new insights into materials design in such systems, which sometimes provide impressively high T_c (viz. electron-doped HfNCl, with T_c=25K).

The quest for new superconductors, ones with high critical temperature T_c or properties more favorable for applications, is gaining in research priority, boosted by discovery of Fe-based superconductors[1] with critical temperature T_c as high as 56 K. The cuprates, followed by MgB_2 and then by the iron pnictides, have illustrated that excellent superconductors appear in surprising regions of the materials palette. The CuO_2 square-lattice cuprates have inspired study of related square-lattice transition metal oxides, such as the "charge conjugate" vanadate[2–4] Sr_2VO_4, the Ag^{2+} material Cs_2AgF_4 [6] that is isostructural and isovalent with La_2CuO_4, and cuprate-spoofing artificially layered nickelates,[5] so far without finding new superconductors.[7,8] These highly interesting materials, though unfruitful for their original intent, illustrate that a more detailed understanding of the mechanism of pairing is a crucial need for a rational search for higher T_c. Nevertheless, materials property design[9] can and does proceed when there is some broad understanding of the mechanism underlying the property.[10–13]

The pairing mechanism is only well understood for electron-phonon coupling (EPC) where MgB_2 with T_c=40 K is most successful so far. The detailed understanding of EPC through strong-coupling Eliashberg theory[14] encourages rational, specific optimization of the EPC strength λ and of T_c, and specific guidelines for one direction for increasing T_c have been laid out.[15]

Recently a new and different class of cuprate, the delafossite structure $CuAlO_2 \equiv AlCuO_2$, has been predicted by Nakanishi and Katayama-Yoshida[16] (NK) to be a $T_c \approx 50$K superconductor when sufficiently hole doped. The calculated EPC strength and character is reminiscent of that of MgB_2, derived from a specific mode (O-Cu-O stretch) and focused in q-space[17–19] due to the circular shape of the quasi-two dimensional (2D) Fermi surface (FS). $CuAlO_2$ is another layered cuprate, with Cu being (twofold) coordinated by O ions in a layered crystal structure. The differences with square-lattice cuprates are however considerable: the Cu sublattice is not square but triangular, and there are *only* apical oxygens. The undoped compound is a d^{10} band insulator rather than a d^9 antiferromagnetic Mott insulator; it is nonmagnetic even when lightly doped, and it is most heavily studied as a p-type transparent conductor.[20] It shares with the hexagonal $\mathcal{T}$NCl system ($\mathcal{T}$=Zr, Hf, with T_c=25.5 K for HfNCl) that doped-in carriers enter at a d band edge. NK provided computational evidence for, but not full calculations of, impressively large λ and high temperature superconductivity T_c up to 50 K when this compound is hole-doped, *viz.* $CuAl_{1-x}Mg_xO_2$. If this prediction could be substantiated, a new and distinctive structural class would be opened up for a more concerted search for high temperature superconductors (HTS).

When our initial linear response calculations indicated weak (rather than strong) EPC, we performed a more comprehensive study. In their work, NK did not carry out linear response calculations of electron-phonon coupling for doped $CuAlO_2$. Instead they made the reasonable-looking simplification of (a) calculating phonons and EP matrix elements for the undoped insulator, (b) doping the system in a rigid-band fashion, i.e. moving the Fermi level E_F as desired, and (c) using those quantities to evaluate q-dependent coupling (λ_q; q includes the branch index) and finally λ, predicting T_c up to 50K. In this paper we provide the resolution to this discrepancy, which involves large spectral weight redistribution due to strong non-rigid-band shifts of spectral density upon doping.

First principles electronic structure calculations were performed within density functional theory (DFT) using the FPLO code[21] to obtain the electronic structure for both undoped and doped materials, the latter one being carried out in the virtual crystal approximation (VCA), where the (say) $Al_{1-x}Mg_x$ sublattice (Ca substitution is also an option) that gives up its valence electrons is replaced by an atom with an averaged nuclear charge. The result is the transfer of x electrons per f.u. from the Cu to the Al layer, corresponding to metallic Cu d^{10-x}. Phonon spectra and electron-phonon coupling calculations for the doped system were performed using ABINIT[22] version 6.6.3 with norm-conserving Trouiller-Martins pseudopotentials. In both codes the Perdew-Wang 92 GGA (generalized gradient approximation) functional[23] was used. The phonon and EPC calculations were done on the

rhombohedral unit cell using a 24^3 k-point mesh and an 4^3 q-point mesh, interpolated to more q-points.

The structural parameters[24] for $CuAlO_2$ used were for rhombohedral R$\bar{3}$m (#166) structure with $a = 5.927$ Å, $\alpha = 27.932°$. This structure is equivalent to $a = 2.861$ Å, $c = 17.077$ Å with hexagonal axes. Cu resides on the $1a$ site at the origin, Al is at the $1b$ site, at $(\frac{1}{2}, \frac{1}{2}, \frac{1}{2})$ and the O atom is in the $2c$ position (x, x, x), $x = 0.1101$.

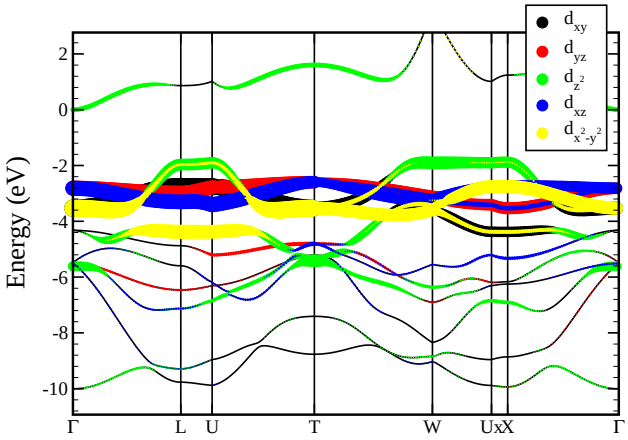

FIG. 1: (color online) Fatbands plot for $CuAlO_2$, with zero of energy at the top of the gap. The size of the symbol represents the amount of $3d$ character, and the color the character as given in the legend.

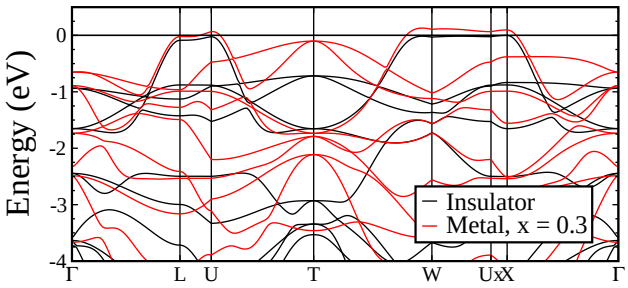

FIG. 2: (color online)Comparison of band structures for the metallic and insulating states of $CuAl_{1-x}Mg_xO_2$ with $x = 0.3$. This moderate level of doping results in very strong changes in the relative band positions.

The band structure of insulating $CuAlO_2$ shown in Fig. 1, which agrees with previous work,[16,25] illustrates that Cu $3d$ bands form a narrow, 2.5 eV wide complex at the top of the valence bands. Oxygen $2p$ bands occupy the region -8 eV to -3 eV below the gap. This compound is a closed shell $Cu^+Al^{3+}(O^{2-})_2$ ionic insulator with minor metal-O covalence, although enough to stabilize this relatively unusual, strongly layered structure.

The upper valence bands providing the hole states consist of d_{z^2} (m_ℓ=0) character with some in-plane d_{xy}, $d_{x^2-y^2}$ (m_ℓ=±2) mixing. The top of this band occurs at the edge of Brillouin zone (BZ) as in, for example, graphene, and is unusually flat along the edge of the

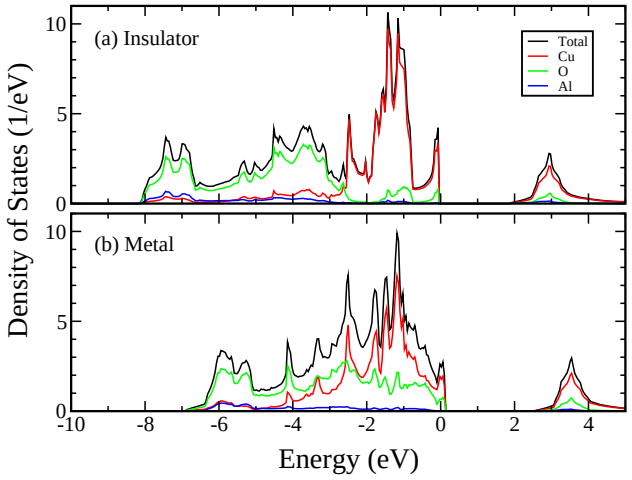

FIG. 3: (color online)Comparison of the density of states for the (a) insulating $CuAlO_2$ and (b) metallic $CuAl_{1-x}Mg_xO_2$ with $x = 0.3$. For the insulator, the Cu d bands are rather separate from the O p bands, but upon doping strong O p permeates the Cu d bands, to near the Fermi level.

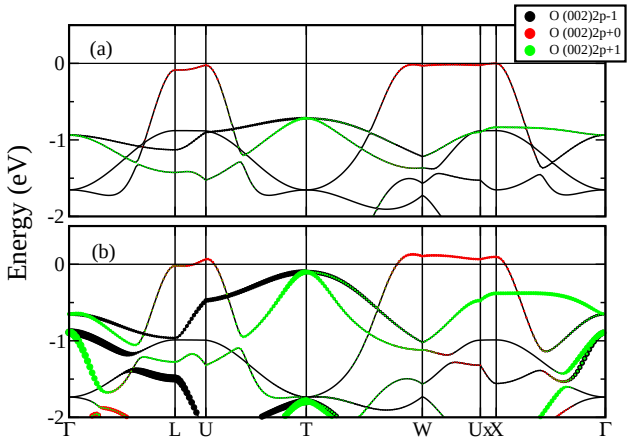

FIG. 4: (color online)Fatband plots for the (a) insulator and (b) x=0.3 metal states, emphasizing O $2p$ character. In addition to the strong shift upward, the O $2p$ character has increased many-fold for the bands near E_F in the metal.

zone, viz. Ux-W (M-K, in hexagonal notation), which comprises all of the edge of the BZ. Since it is also almost dispersionless in the $\hat{z}$ direction, the resulting density of states just below the gap reflects a *one-dimensional phase space*, as shown in Fig. 3a. The $d_{xy}, d_{x^2-y^2}$ bands are nearly flat in the -2 to -1 eV region, and the d_{xz}, d_{yz} bands are even flatter, at -1 to -0.5 eV. These four flat bands reflect very minor d-d hopping in the plane.

When hole-doped, a dramatic shift of spectral weight occurs in the occupied bands, as is evident in Figs. 2 and 3. While the top (d_{z^2}) conduction band hardly changes, the $3d - 2p$ band complex at all lower energies rises rapidly with doping to lower binding energies. The d_{xz}, d_{yz} bands (Fig. 1) acquire considerable $2p$ character and move up to nearly touch E_F at the point T=$(0, 0, \pi/c)$;

further doping will introduce holes into this band. The O $2p$ bands, which lay below the $3d$ bands in the insulator, have shifted upward dramatically by 2 eV (70 meV/% doping), contributing extra screening at and near E_F in the metal. These spectral shifts can be accounted for by a charge-dipole layer potential shift due to the Cu→Al charge transfer. The increased $3d-2p$ hybridization is made more apparent in Fig. 4, which reveals that the d_{xz}, d_{yz} bands at T (and elsewhere) have increased contribution from the O p states. Also apparent in this plot are seemingly extra bands appearing at about -1 eV near Γ; these are bands from below which have been shifted strongly upward by charge transfer.

		Insulator			Metal		
		z^2	xy	x^2-y^2	z^2	xy	x^2-y^2
z^2	t_1	**393**	198	228	**342**	191	220
	t_2	60	8	13	60	14	17
	t_3	**35**	22	25	**59**	17	20
	$t_\perp$	**24**	15	-16	**63**	17	17
xy	t_1		123	117		107	107
	t_2		35	14		36	16
	t_3		11	8		11	10
	$t_\perp$		23	14		31	20
x^2-y^2	t_1			147			140
	t_2 :1			28			27
	t_3			15			17
	$t_\perp$			18			23

TABLE I: Tight binding hopping parameters for insulating and metallic phases, from the three constructed Wannier functions. The labels t_1, t_2, t_3, refer to the first, second, and third neighbor hoppings in the triangular Cu planes. $t_\perp$ refers to hopping between layers. The most significant changes when doped are highlighted in bold print.

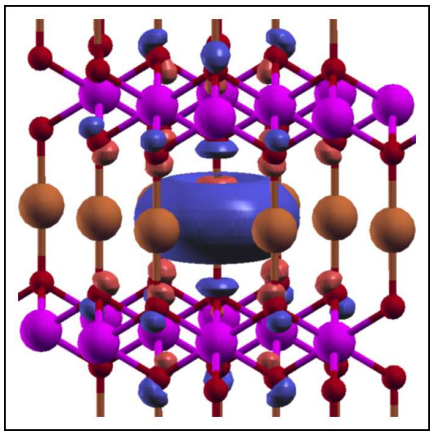

FIG. 5: (Color online.) Isosurface of the Wannier function for the Cu d_{z^2} orbital in the x=0.3 doped metal. Antibonding contributions are seen from the nearest O atoms (small red spheres). The metallic state contains contributions from O ions in the second layer above and below that are not present in the insulator.

More light is shed on the electronic structure of $CuAl_{1-x}Mg_xO_2$ by using Wannier functions (WFs) to construct a tight binding model of the states near the Fermi level. We use the Wannier function generator in the FPLO code.[21] These are symmetry respecting Wannier functions,[26] constructed by projecting Kohn-Sham states onto, in this case, the Cu $3d_{z^2}$, $3d_{xy}$, $3d_{x^2-y^2}$ atomic orbitals, with resulting hopping amplitudes shown in Table I. Hoppings involving the xy and x^2-y^2 orbitals are not significantly different between the insulator and metal. However, hopping amplitudes for the d_{z^2} WF change significantly, the most important being the factor of 2.5 increase in the hopping between layers, $t_\perp$. Consistent with the picture from the DOS, the hoppings for the metallic state are more long-range: nearest neighbor hopping drops by 13%, while third neighbor hopping nearly doubles.

This band dispersion is anomalous for a quasi-2D structure such as this, where normally the $3d$ orbitals with lobes extending in the $x-y$ plane would be expected to be the most dispersive. Instead, it is the d_{z^2} band that disperses, with a bandwidth of 2.5 eV and the band bottom at Γ. Shown in Fig. 5 is the z^2-projected WF for the x=0.3 hole-doped metal. Consistent with their minor dispersion, the WFs for the other $3d$ orbitals (not shown) have little contribution beyond the atomic orbital, showing only minor anti-bonding contributions from nearby O atoms.

The d_{z^2} WF shape is, however, quite unexpected. Although displaying d_{z^2} symmetry as it must, its shape differs strikingly from atomic form. It is so much fatter in the x-y plane than the bare d_{z^2} orbital that it is difficult to see the signature $m_\ell = 0$ "z^2" lobes pictured in textbooks. This shape is due, we think, to "pressure" from the neighboring antibonding O p_z orbitals above and below. There is and (expected) admixture of O $2p_z$ orbitals, as well as a small symmetry-allowed $p_z + (p_x, p_y)$ contribution from the neighboring oxygen ions that finally provides (with their overlap) the in-plane dispersion of the d_{z^2} band. The important qualitative difference compared to the insulator WF is the contribution from O atoms in the *next nearest* planes (across the Al layer) whose states have been shifted upward by the doping-induced charge transfer. This mixing opens a channel for hopping between layers in the Cu d_{z^2} WFs by creating overlap in the two planes of O atoms between Cu layers, it is the source of the increase in $t_\perp$ hopping seen in Table I that leads to the k_z dispersion of the $2p$ band along L-U in Fig. 4 (and more so along Γ-T, not shown), and will promote good hole-conduction in hole-doped delafossites.

Fermi surfaces (FS) are critical to a material once it is doped into a metallic phase. For small hole doping, the FS lies close to the zone boundary everywhere. The FS for $x = 0.3$ hole doping in VCA, displayed in Fig. 6(b), is not so different from that shown by NK for rigid band doping, but the two methods will differ substantially (with new sheets appearing) for larger doping levels, due to the spectral weight transfer. The FS resembles a somewhat bloated cylinder truncated by the faces

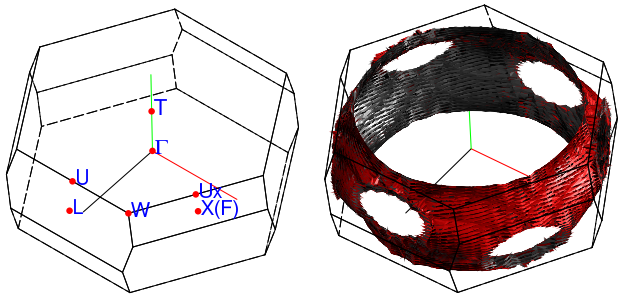

FIG. 6: (color online)Left: rhombohedral zone with special k-points labeled. Right: the sole large multiply-connected Fermi surface for moderately hole doped $CuAl_{1-x}Mg_xO_2$, $x = 0.3$.

of the BZ. The relevant nesting, not necessarily strong, is of two types. A large $2k_F$ spanning wavevector almost equal to the BZ dimension in the $k_x - k_y$ plane will, when reduced to the first BZ, lead to small q scattering on the FS, broadened somewhat by the k_z dispersion. Second, there are "skipping" $\vec{q}$ values along $(\epsilon, \epsilon, q_z)$ for small ϵ. It is for these values of $\vec{q}$ that NK reported extremely strong coupling. We have focused our study of EPC on the regime of doping where NK predicted the very large electron-phonon coupling and high T_c.

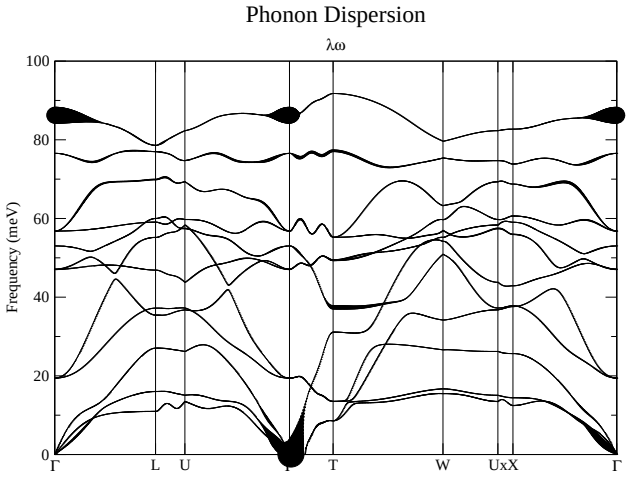

FIG. 7: Phonon dispersion curves for x=0.3 hole-doped $CuAlO_2$, calculated with the ABINIT code on a 8^3 q-point grid with 24^3 k-points. Circles indicate the magnitude of $\lambda_q\omega_q$ for that mode. Some aliasing effects (unphysical wiggles) along L-U and Γ-T are due to the discrete nature and orientation of the q-point mesh.

The phonon dispersion curves calculated from DFT linear response theory are presented in Fig. 7, with fatbands weighting by $\omega_q\lambda_q$ (which is more representative of contribution to T_c than by weighting by the "mode-λ"[27] λ_q alone). Branches are spread fairly uniformly over the 0-90 meV region. Coupling strength however is confined to the Cu-O stretch mode at 87 meV very near Γ, and to very low frequency acoustic modes also near Γ where the density of states is very small. Unlike in MgB_2, this coupling does *not* extend far along k_z; the lack of strong electronic two-dimensionality degrades EPC coupling strength greatly and no modes show significant renormalization. We obtain $\lambda \approx 0.2$, ω_{log}=275K. Using the weak coupling expression $T_c \approx \omega_{log} exp[-1/(\lambda - \mu^*)] \sim \omega_{log} exp(-10)$, no observable superconductivity is expected.

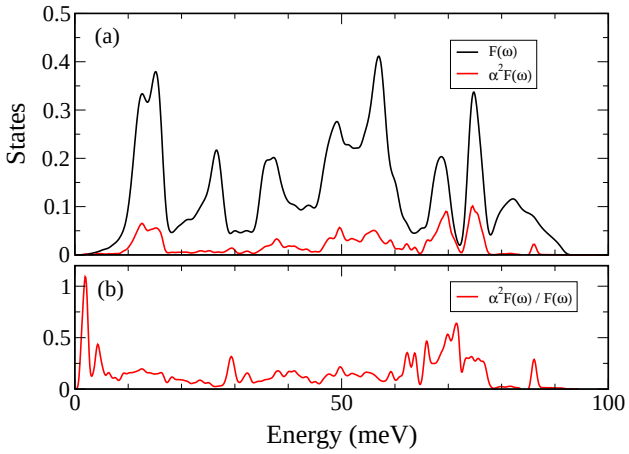

FIG. 8: (a) The phonon density of states and $\alpha^2F(\omega)$ at $x = 0.3$. (b) The quotient $\alpha^2(\omega) = \alpha^2F(\omega)/F(\omega)$ reflecting the spectral distribution of the coupling strength. The peaks below 5 meV are numerically uncertain and are useless for EPC due to the vanishingly small density of states.

Similar to that obtained by NK, the largest electron-phonon coupling arises from the O-Cu-O bond stretch mode. As anticipated from the FS shape, the most prominent contributions arise from small q phonons. There is just visible EPC to phonons near the Brillouin zone face T and along Γ-X and Γ-U. The EPC spectral function $\alpha^2F(\omega)$ is compared in Fig. 8(a) with the phonon DOS $F(\omega)$. As is apparent from their ratio shown in Fig. 8b, the peak around 15 meV is purely from the large density of states there, due to the flat phonon bands over much of the zone at that energy. The coupling with much impact on T_c (*i.e.* area under α^2F) occurs in the 45-70 meV range, and is spread around the zone; however, unlike MgB_2 no frequency range is dominant. The top O-Cu-O stretch move, with the largest λ values and in the 80-90 meV range, are so strongly confined to narrow q ranges that they contribute little to the coupling.

While we conclude, morosely, that high T_c EPC superconductivity will not occur in doped $CuAlO_2$, the behavior that has been uncovered provides important insight into materials properties design beginning from 2D insulators. Hole doping of this delafossite does however provide a new platform for complex electronic behavior. At moderate doping this class provides a single band (Cu d_{z^2}) triangular lattice system, with Cu^{2+} S=1/2 holes, which if coupling is antiferromagnetic leads to frustrated magnetism. The unusual dispersion at low doping, with little dispersion along k_z and also around the zone bound-

ary, leads to an effectively *one dimensional phase space* at the band edge. Another triangular single band transition metal compound[28,29] is $LiNbO_2$, which superconducts around 5K when heavily hole doped[28] and whose mechanism of pairing remains undecided.

This work was supported by DOE SciDAC grant DE-FC02-06ER25794 and a collaborative effort with the Energy Frontier Research Center *Center for Emergent Superconductivity* through SciDAC-e grant DE-FC02-06ER25777. W.E.P. acknowledges the hospitality of the Graphene Research Center at the National University of Singapore where this manuscript was completed.

[1] Y. Kamihara, T. Watanabe, M. Hirano, and H. Hosono, J. Amer. Chem. Soc. **130**, 3296 (1997).
[2] W. E. Pickett, D. J. Singh, D. A. Papaconstantopoulos, H. Krakauer, M. Cyrot, and F. Cyrot-Lackmann, Physics C **162-164**, 1433 (1989).
[3] R. Viennois, E. Giannini, J. Teyssier, J. Elia, J. Deisenhofer, and D. van der Marel, J. Phys.: Conf. Ser. **200**, 012219 (2010).
[4] R. Arita, A. Yamasaki, K. Held, J. Matsuno, and K. Kuroki, J. Phys.: Cond. Matt. **19**, 365204 (2007).
[5] J. Chaloupka and G. Khaliullin, Phys. Rev. Lett. **100**, 016404 (2010).
[6] D. Kasinathan, A. B. Kyker, and D. J. Singh, Phys. Rev. B **73**, 214420 (2006).
[7] S. Kouno, N. Shirakawa, Y. Yoshida, N. Umeyama, K. Tokiwa, and T. Watanabe, J. Phys.: Cond. Matt. **21**, 285601 (2009).
[8] E. Benckiser, M. W. Haverkort, S. Brück, E. Goering, S. Macke, A. Frano, *et al.*, Nat. Matl. **10**, 189 (2011).
[9] N. A. Spaldin and W. E. Pickett, J. Solid State Chem. **176**, 615 (2003).
[10] K. Le Hur, C.-H. Chung, and I. Paul, Phys. Rev. B **84**, 024526 (2011).
[11] E. Coronado, C. Marti-Gastaldo, E. Navarro-Moratalla, A. Ribera, S. J. Blundell, and P. J. Baker, Nature Chem. **2**, 1031 (2010).
[12] V. Pardo and W. E. Pickett, Phys. Rev. B **80**, 054415 (2009).
[13] H. Katayama-Yoshida, K. Kusakabe, H. Kizaki, and A. Nakanishi, Appl. Phys. Exp. **1**, 081703 (2008).
[14] D. J. Scalapino, J. R. Schrieffer, and J. W. Wilkins, Phys. Rev. **148**, 263 (1966).
[15] W. E. Pickett, J. Supercond. Novel Magn. **19**, 291 (2006).
[16] A. Nakanishi and H. Katayama-Yoshida, Solid State Commun. **152**, 24 (2012); *ibid.* **152**, 2078 (2012).
[17] J. An and W. E. Pickett, Phys. Rev. Lett. **86**, 4366 (2001).
[18] Y. Kong, O. V. Dolgov, O. Jepsen, and O. K. Andersen, Phys. Rev. B **64**, 020501 (2001).
[19] J. Kortus, I. I. Mazin, K. D. Belashchenko, V. P. Antropov, and L. L. Boyer, Phys. Rev. Lett. **86**, 4656 (2001).
[20] H. Kawazoe, M. Yasukawa, H. Hyodo, M. Kurita, H. Yanagi, and H. Hosono, Nature **389**, 939 (1997).
[21] K. Koepernik and H. Eschrig, Phys. Rev. B **59**, 1743 (1999).
[22] X. Gonze, J.-M. Beuken, R. Caracus, F. Detraux, M. Fuchs, G.-M. Rignanese, L. Sindic, M. Verstraete, G. Zerah, F. Jollet, *et al.*, Comp. Mat. Sci. **25**, 478 (2002).
[23] J. P. Perdew and Y. Wang, Phys. Rev. B **45**, 13244 (1992).
[24] B. U. Koehler and M. Jansen, Z. Anorg. Allg. Chem. **543**, 73 (1986).
[25] B. J. Ingram, T. O. Mason, R. Asahi, K. T. Park, and A. J. Freemen, Phys. Rev. B **64**, 155114 (2001).
[26] W. Ku, H. Rosner, W. E. Pickett, and R. T. Scalettar, Phys. Rev. Lett. **89**, 167204 (2002).
[27] P. B. Allen, Phys. Rev. B **6**, 2577 (1972).
[28] M. J. Geselbracht, T. J. Richardson, and A. M. Stacy, Nature (London) **345**, 324 (1990).
[29] E. R. Ylvisaker and W. E. Pickett, Phys. Rev. B **74**, 075104 (2006).